Reactive oxygen species-related plasma effects on the apoptosis of human bladder cancer cells in atmospheric pressure pulsed plasma jets

Hea Min Joh, Sun Ja Kim, T. H. Chung, and S. H. Leem

Citation: Appl. Phys. Lett. **101**, 053703 (2012); doi: 10.1063/1.4742742
View online: https://doi.org/10.1063/1.4742742
View Table of Contents: http://aip.scitation.org/toc/apl/101/5
Published by the American Institute of Physics

Reactive oxygen species-related plasma effects on the apoptosis of human bladder cancer cells in atmospheric pressure pulsed plasma jets

Hea Min Joh,[1] Sun Ja Kim,[1] T. H. Chung,[1,a)] and S. H. Leem[2]
[1]*Department of Physics, Dong-A University, Busan 604-714, South Korea*
[2]*Department of Biological Science, Dong-A University, Busan 604-714, South Korea*

(Received 3 May 2012; accepted 23 July 2012; published online 3 August 2012)

Helium/oxygen atmospheric pressure plasma jets driven by pulsed dc voltage with repetition rate of several tens of kilohertz are utilized for plasma-cell interactions. The effect of operating parameters on the apoptosis of cultured human bladder (EJ) cancer cells is investigated. The parameters such as applied voltage, pulse repetition frequency, and duty ratio determine the plasma dose. The apoptotic changes in cells with plasma treatment are detected by staining assay and flow cytometry. Apoptosis rates are observed to correlate well with both the plasma dose and the levels of intracellular and extracellular reactive oxygen species. © *2012 American Institute of Physics*. [http://dx.doi.org/10.1063/1.4742742]

Recently, the research on the applications of atmospheric pressure plasmas has rapidly expanded biology and medicine, the research area called "plasma medicine."[1] The field of plasma medicine includes medical therapies, sterilization, wound healing, and cancer treatment.[2,3] Especially, the use of atmospheric-pressure plasmas in cancer therapies is drawing a great attention because plasmas contain short-lived free radicals including reactive oxygen species (ROS), charged species, and electric field that can induce apoptosis in tumor cells.[4–6] Particularly, atmospheric pressure plasma jets can be utilized in vivo by delivering a lethal dose of plasma to a tumor with the concomitant sparing of surrounding healthy tissues.

Various cancer cells were treated by atmospheric pressure plasma jets, and cellular changes were provoked due to highly active chemical species and electrically charged particles.[4–11] ROS produced by plasma are considered to be the key constituents that induce apoptosis. Plasma treatment induced apoptosis in melanoma cells through a pathway that appears to be dependent on production of intracellular ROS.[12] Apoptotic effects depend on the plasma conditions controlled by many operating parameters including applied voltage, driving frequency, supply gas and flow rate, and treatment time. Thus, the investigation of the effects of operating parameters on apoptosis in plasma-cell interactions would be an important research issue for cancer therapeutic applications of atmospheric plasmas. It is also worth testing directly whether the apoptosis rate induced by atmospheric plasma is related to the intensity of generated intracellular ROS. This paper examines the effect of the parameters such as applied voltage, pulse repetition frequency, and duty ratio of atmospheric pressure pulsed plasma jets on the apoptosis of cultured human bladder (EJ) cancer cells with a focus on the ROS which causes damage to cell membranes and DNA fragmentation in cells participating in the process of apoptosis.

Figure 1(a) shows the schematic structure of the jet device. The plasma jet consists of two electrodes, Teflon fitting, a quartz confinement tube, and a funnel-shaped nozzle. A stainless steel capillary tube was used as the power electrode and its sharp edge allows for the local enhancement of the electric field and, thus, a considerable reduction of the breakdown voltage requirement compared to the plasma jets utilizing the annular ring electrode or dielectric barrier discharge jets, while providing a stable room-temperature operation. Aluminum foil strip was used as the ground electrode. The plasma-forming gas was fed through side of tube, whereas the reactive gas, such as oxygen, was injected through a stainless steel capillary tube.[13] Figure 1(b) illustrates plasma-cell interaction. The plasma was generated by a pulsed dc-driven source with a repetition frequency of several tens of kilohertz (FTLab PDS 4000). The working gas (helium) and the reactive gas (oxygen) flow rate were kept constant at 500 and 5 sccm (cubic centimeter per minute at STP), respectively, otherwise stated. A typical operating condition of the pulsed-dc plasma jet has the applied voltage

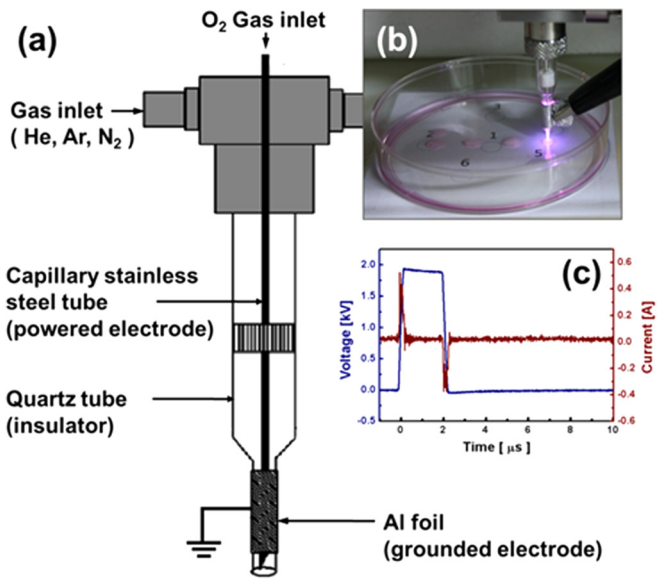

FIG. 1. (a) Schematic presentation of the jet device, (b) photograph of the plasma-cell interaction, and (c) waveforms of applied voltage and total current.

a)Author to whom correspondence should be addressed. Electronic mail: thchung@dau.ac.kr.

1.8 kV, repetition frequency 50 kHz, and duty ratio 10%. Figure 1(c) represents the waveforms of applied voltage and total current.

For the plasma-cell interaction, human bladder cancer cells were cultured in Dulbecco's modified eagle's medium (DMEM) with 10% fetal bovine serum and 100 U/ml penicillin. Cells were incubated at 37 °C with humidified air and 5% CO_2 for 24 h before plasma treatment. EJ cells were seeded in Lab-Tek chamber slides (Nunc™ 177429) for TUNEL (TdT-mediated dUTP Nick-End Labeling) assay with DAPI (4′,6-diamidino-2-phenylindole) or in bioassay dishes (Corning diameter 100 mm) for flow cytometry at a density of 10^5 cells per chamber slide and 10^6 cells per dish, respectively. During the plasma treatment, each dish (or chamber) contained 1 ml (or 0.1 ml for the chamber) of media to prevent cell drying. The cells were exposed for 20 s on 10 points per dish in a distance of 6 mm between nozzle and cell surface.

It was found that the spindle shape of live cells exposed to gas or plasma was changed to the round shape. Detachment of the cells from the extracellular matrix was observed in plasma treated cells and amount of the detached cells increased with increasing treatment time (data not shown). But, no voids were found after treatment of the cell culture with gas flow only (no plasma) at the same conditions.[14] The detachment of the cells depends on the applied voltage and plasma-treatment time. The media including cells were seemingly unchanged by plasma treatment at the applied voltage of 1.2 kV whereas cells were detached at 1.8 kV. The detachment of cell might be attributed to plasma-induced damage of cell adhesion molecules.[15]

To confirm the nuclei undergo apoptosis, the detached cells were collected in Lab-Tek chamber slides. For comparison, non-treated cells were detached using Trypsin 0.25% solution and transferred to chamber slides. And then, they were stained under the TUNEL assay protocol (DeadEnd™ Fluorometric TUNEL System, promega) after 24 hours. The assay measures the fragmented DNA of apoptotic cells. The reattached cells were fixed in 4% formaldehyde and washed in PBS (phosphate buffered saline), after which the cells were stained with TUNEL reaction buffer. The fluorescein-12-dUTP labeled DNA can then be either visualized directly or by fluorescence microscopy. The emitted green fluorescence of apoptotic cells were observed under Laser Scanning Confocal Microscope (Carl Zeiss LSM 510). Figure 2 represents the merging view of the blue fluorescence of DAPI staining and the green fluorescence in fluorescein-12-dUTP fluorescence images for the untreated cells (detached by Trypsin) (Fig. 2(a)) and plasma-treated cells (Fig. 2(b)). Compared to the non-treated cells, the detached cells by the plasma exposure showed a localized green fluorescence of apoptotic cells in a blue background. It is also observed that the plasma-treated cells exhibit the apoptotic fragmentation. This can be considered as clear evidence that detached cells by plasma exposure undergo apoptosis.

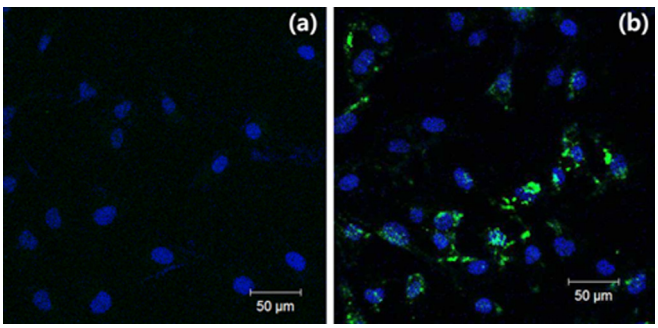

FIG. 2. Confocal microscope images of the detached EJ cells stained with the TUNEL assay and DAPI: (a) non-treated cells (detached by Trypsin) and (b) plasma treated cells.

At least 20 h after treatment, the percentage of apoptotic cells were determined by flow cytometry using Annexin V-Fluorescein isothiocyanate (FITC) apoptosis detection kit (BD Biosciences 556547). Non-treated and plasma-treated cells were harvested, washed with PBS and resuspended in 1× binding buffer containing Annexin V and propidium iodide (PI). After incubation for 20 min at room temperature in the dark, fluorescence-activated cells were detected using a 4-color flow cytometric analyzer (Beckman Coulter Epics XL), and the data were analyzed using EXPO32 flow cytometry software. The percentage of cell number was counted by flow cytometry using FITC Annexin V and PI staining as shown in Figure 3. In all compared samples, the number of counted events is 10^5. The upper figures represent apoptotic stages in cancer cells induced by plasma exposure. The quadrant I, II, III, and IV denote necrotic, late apoptotic, viable, and early apoptotic regions, respectively. The results were obtained in the pulsed dc plasma jet with different conditions: (a) non-treated control, (b) 500 sccm helium with the 5 sccm of oxygen (helium/oxygen) plasma at the applied voltage 1.2 kV, repetition frequency 50 kHz, duty ratio 10%, and the amount of working media in the dish 1 ml, (c) helium/oxygen plasma at 1.8 kV, 50 kHz, 10%, 1 ml, (d) helium/oxygen plasma at 1.8 kV, 20 kHz, 10%, 0.5 ml, and (e) helium/oxygen plasma at 1.8 kV, 50 kHz, 10%, 0.5 ml.

Lower figures include the graph (f) showing the ratios of apoptosis and necrosis for different gas flows and applied voltages (untreated control, a weak gas flow only (gas 1; 100 sccm, exposure time 10 s), a medium gas flow only (gas 2; 500 sccm, exposure time 20 s), 1.2 kV, 1.5 kV, and 1.8 kV), the graph (g) comparing the apoptosis rates for different pulse repetition frequency (20 kHz and 50 kHz), the graph (h) comparing the apoptosis rates for different pulse duty ratios (10% and 50%), the graph (i) comparing the apoptosis rates for different amount of working media (0.2 ml, 0.5 ml, and 1.0 ml), and the graph (j) comparing the apoptosis rates for different flow rates of helium and additive oxygen (helium: 100 and 500 sccm, oxygen: 5, 10, 20 sccm). As shown in the figures, the incidence of apoptotic cells was significantly enhanced in plasma-treated cells. It was noted that the percentage of apoptotic cells was increased from 24.15% in ((b): 1.2 kV) to 30.05% (1.5 kV) and 31.48% in ((c): 1.8 kV) with the applied voltage. It should be noted that the treatment with a weak gas flow only did not affect apoptosis rates compared to the untreated control, while a medium gas flow resulted in quite a large apoptosis rate. This can be explained from that the cellular changes can occur since the physical shear stress imposed by the gas flow could possibly deliver a shearing force to the adherent cells to peel them off from the substrate[15] and that the detached cells by physical stress may

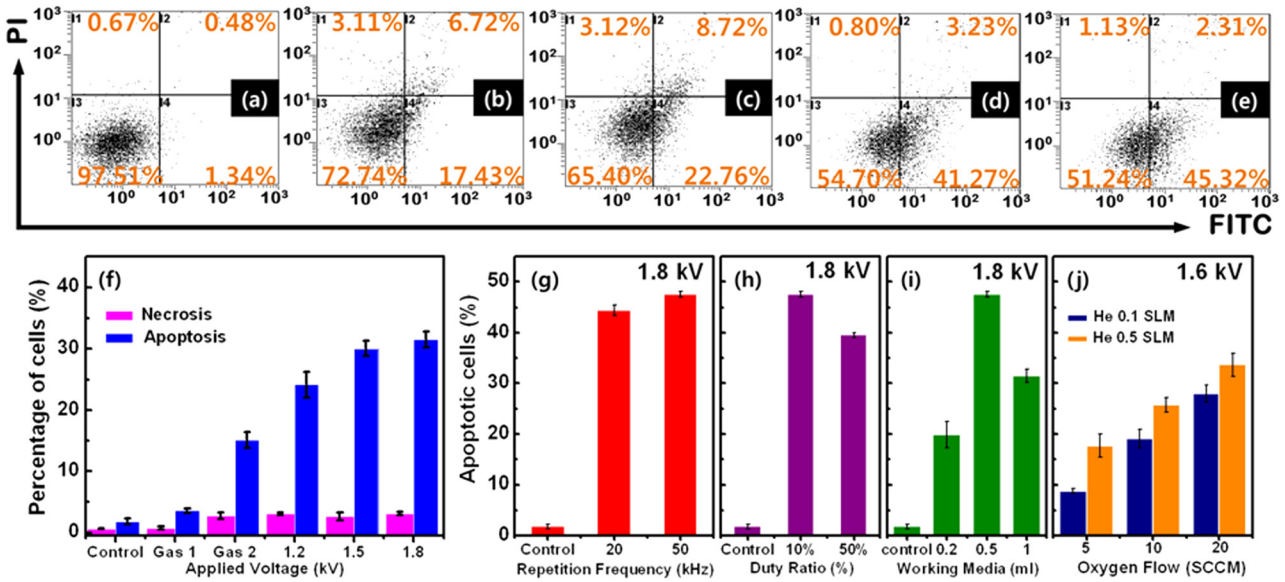

FIG. 3. The apoptosis stages (the upper figures) obtained for different conditions of the plasma-cell interactions: (a) non-treated control, (b) 500 sccm helium with the 5 sccm of oxygen (helium/oxygen) plasma at the applied voltage 1.2 kV, repetition frequency 50 kHz, duty ratio 10%, and the amount of media in the dish 1 ml, (c) helium/oxygen plasma at 1.8 kV, 50 kHz, 10%, 1 ml, (d) helium/oxygen plasma at 1.8 kV, 20 kHz, 10%, 0.5 ml, and (e) helium/oxygen plasma at 1.8 kV, 50 kHz, 10%, 0.5 ml. The bottom figures are the comparisons of the ratios of apoptosis for different operating parameters: (f) applied voltage (comparison with untreated control, a weak (gas 1), and a medium (gas 2) gas flow only), (g) pulse repetition frequency, (h) duty ratio, (i) amount of working media, and (j) flow rates of helium and additive oxygen.

undergo apoptosis. The percentage of apoptotic cells increased from 44.50% in ((d): 20 kHz) to 47.63% in ((e): 50 kHz) with increasing pulse repetition frequency, and increased from 39.59% (not shown (duty ratio: 50%)) to 47.63% in ((e): 10%) with decreasing duty ratio, respectively. It is well known that the plasma plume current increases with applied voltage and driving frequency. In our previous study,[16] it was also observed that the plasma ignition is easier, and the volume and luminosity of plasma bullet increase with a decrease in the duty ratio. All these observations indicate that apoptotic effect is plasma-dose dependent. The graph (i) reveals that apoptosis rate depends on the amount of media. Medium contains many different materials, and various secondary effects due to the interaction between plasma and medium may occur. This may also be related to the penetration depth of plasma species into the cell. The optimal amount of media provides effective interaction with plasma jet, while protecting cells from desiccation.[14]

Next, we investigated the effect of additive oxygen on the apoptosis rate. To produce more radials in the gas phase, oxygen gas was injected into the capillary tube while helium was fed through the quartz tube.[17] In order to minimize the gas flow effect, the flow rate of helium was reduced to 100 sccm and the applied voltage and plasma treatment time were adjusted to 1.6 kV and 10 s to prevent the cell detachment. As shown in Fig. 3(j), the apoptosis rate is observed to increase with the additive oxygen flow. This trend is more predominant at lower flow rate of helium.

The intercellular generation of ROS after plasma treatment was detected by a flow cytometry analysis and by fluorescence microscopy using 2′-7′-dichloro fluorescein diacetate (DCF-DA). The assay employs the cell-permeable fluorogenic probe DCF-DA (Molecular Probes®), which diffuses into cells and is deacetylated by cellular esterases to the non-fluorescent DCFH. In the presence of ROS, DCFH is rapidly oxidized to highly fluorescent DCF.[18] Generation of ROS can be detected by monitoring the increase in fluorescence. Fluorescence was measured with excitation and emission wavelengths set at 488 nm and 520 nm, respectively. EJ cells (10^6 cells) in bioassay dishes (Corning diameter 60 mm) were pretreated with 20 μM DCF-DA for 30 min at 37 °C in the dark. Then, cells were exposed helium/oxygen plasma (and/or gas flow only) for 10 s on 9 points per dish and incubated for 30 min. The 300 μM N-acetyl-cysteine (NAC), which has been used as an anticancer agent in preclinical models, was used as ROS scavenger. According to the manufacturer's protocol, cells were harvested and washed with PBS. Fluorescence-activated cells were detected and analyzed using a flow cytometer (Beckman Coulter Epics XL) and fluorescence microscopy (Motic AE31). Figure 4 shows the fluorescence images and FL1 fluorescence histograms of intracellular ROS generation. Control cells were stained with DCF but the fluorescence intensity was much lower (Fig. 4(a)), whereas plasma-treated cell populations containing high levels of DCF fluorescence were increased with applied voltage (Figs. 4(b) and 4(c)). Likewise, the number of detected cells after plasma treatment was increased as shown in Figs. 4(d)–4(f). It is observed that plasma exposure leads to the increase of the intracellular ROS generation and plasma-induced ROS production can be controlled by plasma dose.

To confirm the extracellular ROS in the plasma, optical spectra were recorded for emission along the axis of the jet in the wavelength range from 200 to 900 nm. Figure 5(a) shows the emission spectrum observed in the plasma jet for a typical operating condition. The emission spectrum reveals the presence of excited helium, atomic oxygen, and some excited air molecules. The variations of the intensities of NO, OH, O, and $H_\alpha$with the operating conditions of the pulsed dc driven source are observed in Fig. 5(b). The case

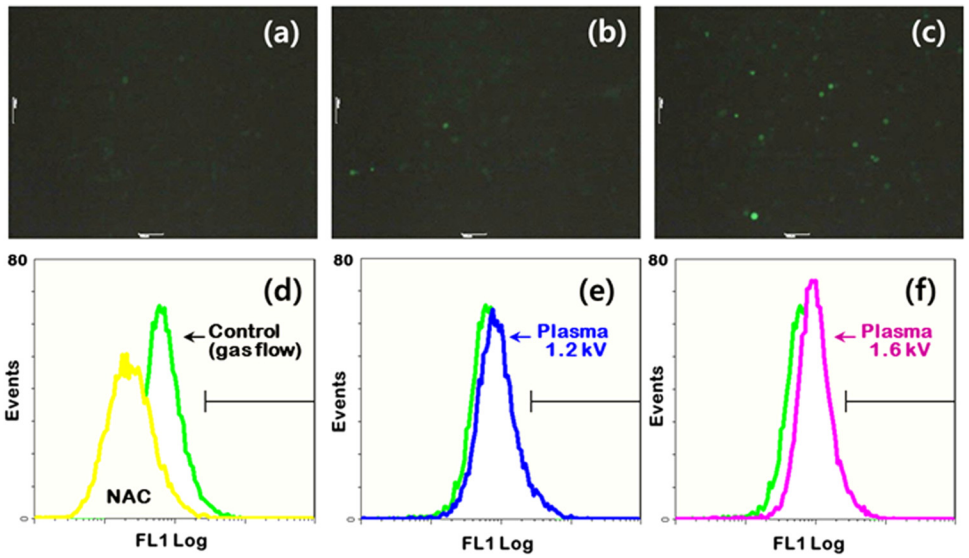

FIG. 4. Intracellular ROS effects: fluorescence microscope images ((a), (b), (c)) and the FL1 fluorescence histograms (number of events over fluorescence intensity) ((d), (e), (f)) of control cells (gas flow only), plasma-treated cells at 1.2 kV, and plasma-treated cells at 1.6 kV, respectively.

of pulsed dc voltage at 1.8 kV (repetition rate of 50 kHz and 10% duty ratio) exhibits an enhanced intensity level of highly reactive oxygen radicals such as OH, NO, O, and H_α compared to the spectra of others. Earlier study also showed that OH and O radicals increase with the addition of oxygen.[8] Since the ROS is in general associated with the induction of cell death, the richness of these species may make this operating condition produce better apoptotic rate.[11] As can be seen in Fig. 3, the incidence of apoptotic cells was more increased at this operating condition. This is closely related to the increase in the ROS level. It can be stated that the primary role in the apoptosis is played by reactive oxygen species such as NO, OH, O species in the plasma plume and that the apoptosis rate depends on the amount of ROS which is influenced by plasma dose and other operating parameters. These data suggest that the generation of intracellular ROS and the induction of apoptosis are the results of plasma's interaction with the extracellular medium and that the effects of plasma depend on the plasma dose and the concentration of active species in the medium.

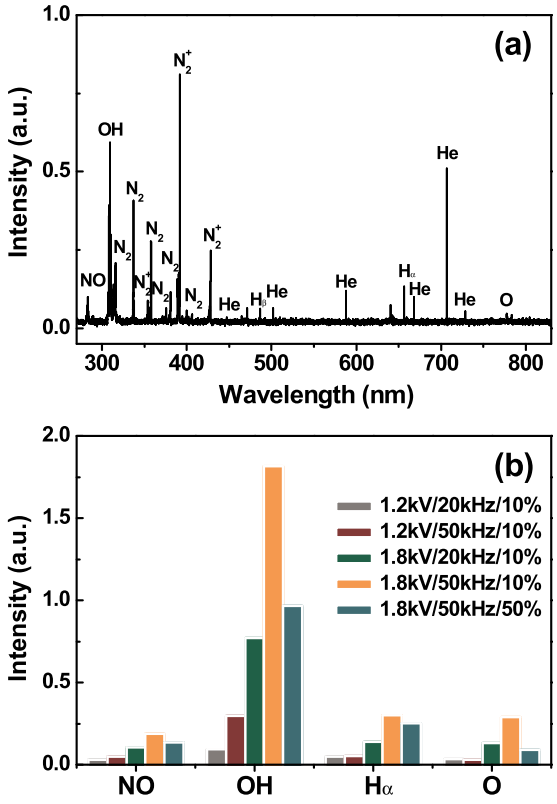

FIG. 5. (a) Emission spectra from observed in the helium/oxygen plasma for the pulsed dc-driven source (1.6 kV, 50 kHz, 10%, 500 sccm). (b) Comparison of the emission intensities from NO_y, OH, H_α, O radicals for different operating conditions.

In conclusion, the potential of plasma jet for inducing apoptosis in human bladder cancer cells was evaluated. The TUNEL assay and DAPI showed that the detached cells underwent apoptosis. Apoptosis rate correlates well with both the plasma dose and the levels of intracellular and extracellular ROS. This observation fully supports the prospect of utilizing atmospheric pressure plasma jets as a promising cancer therapy.

This work was supported by the National Research Foundation of Korea under Contract No. 2012002591.

[1]A. Fridman, A. Chirokovo, and A. Gutsol, J. Phys. D: Appl. Phys. **38**, R1 (2005).
[2]G. Fridman, G. Friedman, A. Gutsol, A. B. Shekhter, V. N. Vasilets, A. Fridman, Plasma Process. Polym. **5**, 503 (2008).
[3]M. Laroussi, IEEE Trans. Plasma Sci. **37**, 714 (2009).
[4]G. J. Kim, W. Kim, K. T. Kim, and J. K. Lee, Appl. Phys. Lett. **96**, 021502 (2010).
[5]S. Kalghatgi, C. M. Kelly, E. Cerchar, B. Torabi, O. Alekseev, A. Fridman, G. Friedman, J. Azizkhan-Clifford, PLoS One **6**, e16270 (2011).
[6]J. Y. Kim, Y. Wei, J. Li, P. Foy, T. Hawkins, J. Ballato, and S.-O. Kim, Small **7**, 2291 (2011).
[7]E. Stoffels, I. E. Kieft, R. E. J. Sladek, L. J. M. van den Bedem, E. P. van der Laan, and M. Steinbuch, Plasma Sources Sci. Technol. **15**, S169 (2006).
[8]X. Zhang, M. Li, R. Zhou, K. Feng, and S. Yang, Appl. Phys. Lett. **93**, 021502 (2008).
[9]J. Y. Kim, S.-O. Kim, Y. Wei, and J. Li, Appl. Phys. Lett. **96**, 203701 (2010).
[10]K. Kim, J. D. Choi, Y. C. Hong, G. Kim, E. J. Noh, J.-S. Lee, and S. S. Yang, Appl. Phys. Lett. **98**, 073701 (2011).
[11]S. J. Kim, T. H. Chung, S. H. Bae, and S. H. Leem, Appl. Phys. Lett. **97**, 023702 (2010).

[12]R. Sensenig, S. Kalghatgi, E. Cerchar, G. Fridman, A. Shereshevsky, B. Torabi, K. P. Arjunan, E. Podolsky, A. Fridman, G. Friedman, J. Azizkhan-Clifford, and A. D. Brooks, Ann. Biomed. Eng. **39**, 674 (2011).
[13]H. S. Park, S. J. Kim, H. M. Joh, T. H. Chung, S. H. Bae, and S. H. Leem, Phys. Plasmas **17**, 033502 (2010).
[14]A. Shashurin, M. Keidar, S. Bronnikov, R. A. Jurjus, and M. A. Stepp, Appl. Phys. Lett. **93**, 181501 (2008).
[15]B. Gweon, D. B. Kim, D. Kim, H. Kim, H. Jung, J. H. Shin, and W. Choe, Appl. Phys. Lett. **99**, 063701 (2011).
[16]S. J. Kim and T. H. Chung, IEEE Trans. Plasma Sci. **39**, 2280 (2011).
[17]V. Leveille and S. Coulombe, Plasma Sources Sci. Technol. **14**, 467 (2005).
[18]T. M. Johnson, Z. X. Yu, V. J. Ferrans, R. A. Lowenstein, and T. Rinkel, Proc. Natl. Acad. Sci. U.S.A. **93**, 11848 (1996).